Turki Alamro [ID],[1] Mohammed Yunus [ID],[1] Rami Alfattani [ID],[1]
Ibrahim A. Alnaser[2]

Effect of part build orientations and sliding wear factors on tribological characteristics of FDM processed parts

Fused Deposition Modeling (FDM) components are commonly used for either prototypes or end products, mostly made of polymers. Polymers offer low frictional resistance to wear, so most of the engineering polymers find their increased usage in day-to-day industrial as well as domestic needs. The influence of many process controlling elements on the mechanical part properties is already being studied extensively, which demands the study of tribological characteristics like friction and wear rate under varying normal load (NL), sliding velocities (V) and part building orientations (PBO). The results showed a significant impact of the PBO and NL at various V on the tribological properties under various significant suitable sliding circumstances. Cracks were formed in the cylindrical tribometer specimens of Acrylonitrile butadiene styrene (ABS) fabricated at low PBO when operated at high NL, and V. Vertical PBO to the FDM building platform in the layers form where a number of inter-layers can bear maximum NL at higher values of V resulted in uniform wear and low frictions. Friction was noticed very low at minimum NL when PBO was $0°$ (horizontal) and $90°$ (vertical), but increased at high NL between PBO of $15°$ to $60°$. The FDM parts improved compared to those from conventional manufacturing processes.

1. Introduction

Additive manufacturing (AM) systems utilize 3D CAD models to produce final components/products directly, with components being built on additive rules. Conversely, conventional production techniques utilize subtractive rules on raw

---

✉ Mohammed Yunus, e-mail: myhasan@uqu.edu.sa

[1] Department of Mechanical Engineering, Umm Al-Qura University, Makkah City, Saudi Arabia.
ORCIDs: T.A.: 0000-0001-7520-9181, M.Y.: 0000-0003-1116-4978, R.A.: 0000-0003-1180-8040

[2] Mechanical Engineering Department, King Saud University, Riyadh, Saudi Arabia.

substances to build such final component/products. AM offers significant advantages such as manufacturing complex/intricate geometries, zero tooling, as well as no human intervention and single setup manufacturing. During the past decade, AM has attracted massive attention in developing products to meet the expectations of both designers and manufacturers across various industries, ranging from manufacturing to medical and automotive concept development [1]. Fused deposition modeling (FDM) is one widespread AM technique where filaments are deposited in a layer form, and layers over layers are then added to fabricate the final component/product. This relatively new and yet already commonly used production method is used to develop a component/product by scanning its descriptions through a 3D CAD model [2]. Besides the ease of operation, including the capability to build components with local structured properties and varied materials, FDM has resulted in manufacturing parts for prototyping and functional components. The FDM process's fabrication components require less time when compared to conventional production methods and directly produce substantial samples utilizing geometric information. Hence, the term "Rapid Prototyping" (RP) is used in a product development context to refer to technologies such as FDM. Today, many RP parts are directly used as actual production products, which requires a new understanding of prototyping [3, 4].

Among the different AM technologies, the predominant techniques are stereolithography (SLA), FDM, layered part production (LPP), 3D Printing, etc. [5–7]. Parts manufactured through AM technologies must initially be modeled using 3D CAD software and generated file (STL form) transferred to AM machine, and machine set-up for building the part pattern are set by a sliced 3D model. Part removal and post-processing as sandblasting, painting, or coating may be performed based on the specific use requirements before the created part is then put to its intended use [8].

Since polymers and their composites offer very low friction, many polymers are currently used in non-wet sliding circumstances, i.e., where no lubrication is needed. The extensive utilization and common usage of polymers as final products have led to comprehensive research on its tribological properties such as friction and wear-out techniques [9, 10]. Polymers used in engineering applications are subjected to wear out by the sliding action of sample pins at varying velocities against their mating surface of a hardened steel disc/wheel, the roughness of the contacting surfaces, and its orientation. Increasing the contacting surface's roughness has led to an improve wear rate with changing properties for various polymer types. When the average surface roughness factor (Ra) was very low, the waviness of the surface orientated parallel to the sliding path resulted in a higher wear rate than that of the waviness placed perpendicular to the sliding path. The inclination of the surface's waviness on a ground contacting surface regarding the sliding path impacts the wear rate with unoccupied polymers.

In prior research, molds produced employing rapid tooling techniques for epoxy-resin based composites were studied to evaluate thermal conductivity (K)

and wear-out resistance. Simultaneously, metallic fillers allow for major improvements in the K value of the resin and wear resistance of milled fibers [11]. Tribological tests were conducted using pure resin, a resin filled with aluminum (Al), tri-phase composites made up of epoxy, Al elements, and pulverized fibers of glass or carbon [12]. The properties of friction and sliding wear of a number of polymers (poly-amide-66, poly-phenylene-sulfide, and poly-tetra-fluoro-ethylene) under dry and wet (oil-lubricated) conditions employing a pin-on-disc (PD) tribometer by varying NL and V combinations were studied. Frictional characteristics for factor combinations were greatly enhanced, and wear-out resistance properties of poly-phenylene-sulfide, and poly-tetra-fluoro-ethylene were enhanced but were decreased for poly-amide-66 through lubrication. Fictional heat was created to change the condition of polymer mating surfaces that significantly affected the tribology responses of polymer's contacting surface combinations in dry sliding circumstances. Because oil lubrication dissipates frictional heat, adhesive wear was used in dry conditions. Conversely, adhesive wear combines with erosive wear to form a new wear-out mechanism in a lubricated state [13].

The parametric dependency of the FDM process on tribological properties, such as wear and friction, causes that finished products should have better tribological properties.

As increasingly more parts are manufactured using FDM – not only in RP but also in final products – it is important to be aware of this dependency during the design stage before moving on to manufacturing the products. Apart from their commercial use, FDM products are also used in many biological and biomedical applications [14, 15]. The manufacturing of complex parts, easiness of product visualization, cost-effectiveness, time-efficient manufacturing, and inexpensive tooling are only some of AM manufacturing's advantages over traditional manufacturing. With increasing demand created by industrial and customer needs, challenges remain from the concept generation through the design stage to final manufacturing [16–19].

In this work, we investigated the correlation between the coefficient of friction (COF), the running-in distance, and the wear properties of acrylonitrile butadiene styrene (ABS) polymer by comparing a 3D printed internal triangular flip ABS pin with a 3D printed solid ABS pin under varying loads and sliding speeds. A triangular flip internal structure was manufactured via 3D printing through fused filament fabrication (FFF). This showed a lower COF and exhibited early contact microstructure effects as well as changes in the surface area composition. A morphological analysis revealed that delamination and abrasion were the main mechanisms of wear [20].

To increase wear resistance and reduce water absorption and friction in underwater applications that use reinforced composites, and at the same time to improve hardness and moisture repelling ability, the epoxy matrix is reinforced with waste plastic particulates and filled with seashell powders. The results are then analyzed

to identify which parameters influence the composites' water absorption and wear properties [21].

Current literature suggests that AM technologies offer a synergy that favors product/prototype properties improvement. With the growing application of these AM technologies in various fields of science and technology, ranging from tooling, automotive, medical implants, and food processing to tissue engineering, substantial efforts have been devoted by many researchers to understand and adapt these technologies accordingly. FDM is one technology in which the possibility of process improvement has been limited. Due to its inherent advantages, including low material cost, readily available raw material, and manufacturing custom properties, FDM has seen a greater use than any other AM technologies. Parts manufactured using the FDM process, like others made with an AM machine, display diverse properties. As any evolving technology, the AM has its merits and shortcomings. Then, it is essential to primarily overcome the limitations through better understanding of the process and to analyze the related process parameters that affect the process quality.

Parts produced by FDM consist of ABS polymers, which offer good wear resistance, strength, and dimensional stability have not been probed. Little to no research exists to understand the TP of FDM-fabricated components. There is a need to investigate various FDM process settings that affect the tribological properties (TP) of ABS-made parts in the FDM process. This study seeks to understand the effect of FDM variables, such as normal load, sliding velocities, and the orientation of the part construction direction on wear-out rate and friction coefficient, utilizing a standard PD tribometer.

2. Methods and materials

For the FDM process, a uPrint 3D printer is used to fabricate test samples by extruding ABS filament. The other material carrier is primarily a water-soluble material for supporting the model during the building process which has to be removed completely once the part is completed. The building and the support materials are in the spools form held in a carrier. The semi-molt material is deposited in the form of filaments thus forming layers. The available layer resolution is 0.254 mm with a minimum wall thickness of 0.914 mm. A suitable part infill/model interior can be chosen based on need. To manufacture the specimen in uPrint, the specimens can be modeled in any solid modeling software and imported to the Dimensional Catalyst software, the user interface for the uPrint 3D printer. Once the test specimens are arranged as required in the model space of the software, with respect to the orientation in different directions including horizontal and vertical, they can be manufactured by submitting the CAB file to the 3D printer. Once the test specimens are built, they are placed in a solution chamber to remove the support material. The specimens are then dried and readied for the testing. In FDM, the model material/build material, i.e., ABS P400 polymer, is

heated to near its melting temperature and deposited layer upon layer. Two separate liquefier-nozzle assemblies are arranged in the extrusion head, one for the model material and the second one for the support material. Current literature also identifies that the FDM process parameter settings play a dominant role, determining the properties of the part. From a designer and manufacturer's point of view it is crucial to study the effects of these process parameters on the final quality desired for the parts/prototypes that are produced. The use of experimental design techniques would provide the best possible results assuming detailed knowledge of the process parameters and understanding their effect on the wear and frictional properties.

For defining TP such as wear rate (W_r) and friction coefficient (COF) of FDM-processed components, the Ducom^{TM} PD tribometer was used. The impact of process variables of both the FDM system and the PD tribometer on the parts manufactured by the FDM process as well as on TP (W_r and COF) was assessed. The parameters used to study and estimate the TPs are normal load (NL), sliding velocity (V), and part/pin building orientation (PBO) during the FDM process are specified in Table 1, while other factors are treated as fixed, of standard values. Based on the preceding works, practices, and real engineering applications, the manufacturer-recommended permitted values of variables were considered in this work. The pins of ABS material were manufactured using the Prusa I3 MK3, a variant of the FDM machine. The parts were manufactured using the variables in Table 1 to observe the effect of PBO, NL, and V variables [22]. For the present work, the applied NL values are 5–30 N at 5 N steps; the used sliding velocity, V values are 0.5, 1, 1.5, 2.25 and 3 m/s with the sliding distance of 2 km. The PD was used to carry out trials to estimate the friction coefficient and wear rate of ABS samples conducted at ambient room temperature and in dry conditions were made of high-hardened carbon steel with high compressive strength and abrasion resistance alloy and quite often employed as wear resisting machine elements used as the wheel/disc substance. It had a roughness of 0.30–0.35 μm and was used for the disc. The surface of the disc was cleaned before each test using emery paper to reliably measure the weight loss. Because the worn-out material is a polymer which insignificantly affects surface roughness of the disc (the disc is made of a harder material), it does not need to be checked for maintained surface roughness.

Table 1.

FDM and PD variables and their values

Factor	Name	Factor Settings						
NL	Normal load (N)	5	10	15	20	25	30	–
V	Sliding velocity (m/s)	0.5	1	1.5	2.25	3	–	–
PBO	Pin building orientation (degrees)	0	15	30	45	60	75	90

2.1. Estimation of wear rate (W_r) and friction coefficient (COF)

The COF is calculated using frictional twisting measured using a load cell tachometer mounted on the PD equipment. The wear rate in terms of wear volume (W_v) measured through material loss of the pin volume is equal to the volume of the cone's frustum, as specified in Eq. (1). The wear rate K (mm^3/Nm) reported in this study is calculated according to Eq. (2):

$$W_v = \frac{(\pi \cdot \Delta h) \cdot (PD_1)^2 + (PD_2)^2 + (PD_1 \cdot PD_2)}{3}, \tag{1}$$

$$W_r = \frac{W_v}{L \cdot F}, \tag{2}$$

where Δh is the height of material removed, PD_1, PD_2 are the pin's radii before and after the wear test, and h is the difference in heights before and after the test, as shown in Fig. 1. L is the distance traveled by the disc with a pin sliding over it; in this study, L is set to 2500 m. F is the load applied during the test. The chosen load is very small when compared to that of metal specimens to avoid a buckling of the pin. Based on the configuration settings obtained from the ASTM-D99 standards, pins for the PD test are manufactured using the FDM process, and the tests are conducted on the PD machine for all the experimental runs. The friction coefficient and wear rate are evaluated and tabulated as demonstrated in Appendix A.
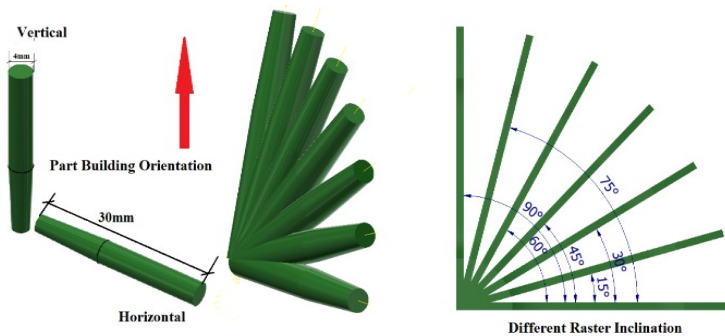

Fig. 1. Pin sample used in the PD experimental set-up

3. Results and discussion

3.1. Friction coefficient (COF)

In FDM, the crude substance in the solid strand form is heated to a semi-molten state while passing to move through the extruding head and is deposited on the building platform from a nozzle layer over a layer, which results in a staircase effect. Due to this, FDM components never exhibit a smooth surface

quality/finish and the polishing of pins/FDM samples becomes necessary for most FDM part applications. This is performed on a two-wheel polishing machine to create appropriate contacting surfaces between the pins and the wheel. It ensures that the pins surface quality lies within the limits that allow one to develop and maintain good mating with the wheel. During the test, as the test duration increases, the friction remains uniform for a certain period because of intrinsic frictional properties. However, due to consistent wear the solid-state material of ABS sample turns into powder. This decreases the COF repeatedly until it attains a steady and constant value. Only after ample time, when the high spots developed at the contact surfaces are levelled off, COF is reduced and stabilizes [9]. This gradual surface destruction is depicted in Fig. 2h showing the variation of COF with total trial time. Figs 2a-2g show that the factors which predominantly affect the friction coefficient are a combination of orientation of the filaments of the FDM machine with V and NL.

Figs 2a–2h show the effect of the NL with V at PBO of 0° (horizontal), 15°, 30°, 45°, 60°, 75°, and 90° (vertical) directions on the COF. When increasing either NL or V, the COF first increases as high spots develop on the contacting surfaces and then – with V lower or equal to 1.5 m/sec – reduces gradually. This reaction can be commonly observed with most polymers [11]. When PBO or filament orientation increases from lowermost value of 0° to the near mid value of 38°, COF increases. COF decreases with the increase of V beyond PBO of 38° because the surface layers of the sample have a tendency to become flat on the wheel surface. Additionally, uniform wear-out down the cross-section of the stratum occurs, which in turn reduces COF [12, 13]. However, beyond V = 1.5 m/sec – and especially at 3 m/sec – COF continues to increase as these polymers do not withstand greater values of V under higher loads. They exhibit a higher wear rate; and in turn they increase COF gradually to maintain contact between the wheel surface and the sample surface. COF decreases if the test duration is prolonged, due to flattening the existing unevenness of high spots at contacting surfaces. However, the surface cannot be totally flattened/smoothed [23]. Therefore, COF stagnates at a value of 0.29 after 2000 seconds, as shown in Fig. 2h. Figs 2a–2g show that the COF is smaller when wires/filaments are built up at maximum PBO (or orientation of base for building a part) irrespective of variation of V and NL when correspondingly compared to each other. Therefore, the increasing V of wheel will cause the layers of part be flat to wheel surface and a constant wear due to the flattened or smoothed profiles of each layer of the sample pin reduces COF. With increasing time, the roughness austerities reduced without their complete disappearance. Conversely, the situation can be perceived as reducing the PBO or the feeding wire inclination. The deposited filament thread is approaching a parallel to the build plane, where the wheel's V and NL have shifted the previous rough portion of the filament, causing an increase in COF. Similarly, an increasing NL develops the cracks between the layers. A similar behavior can also be observed with the varying NL and V of the wheel for different PBO conditions. It provides optimal values of parameters to
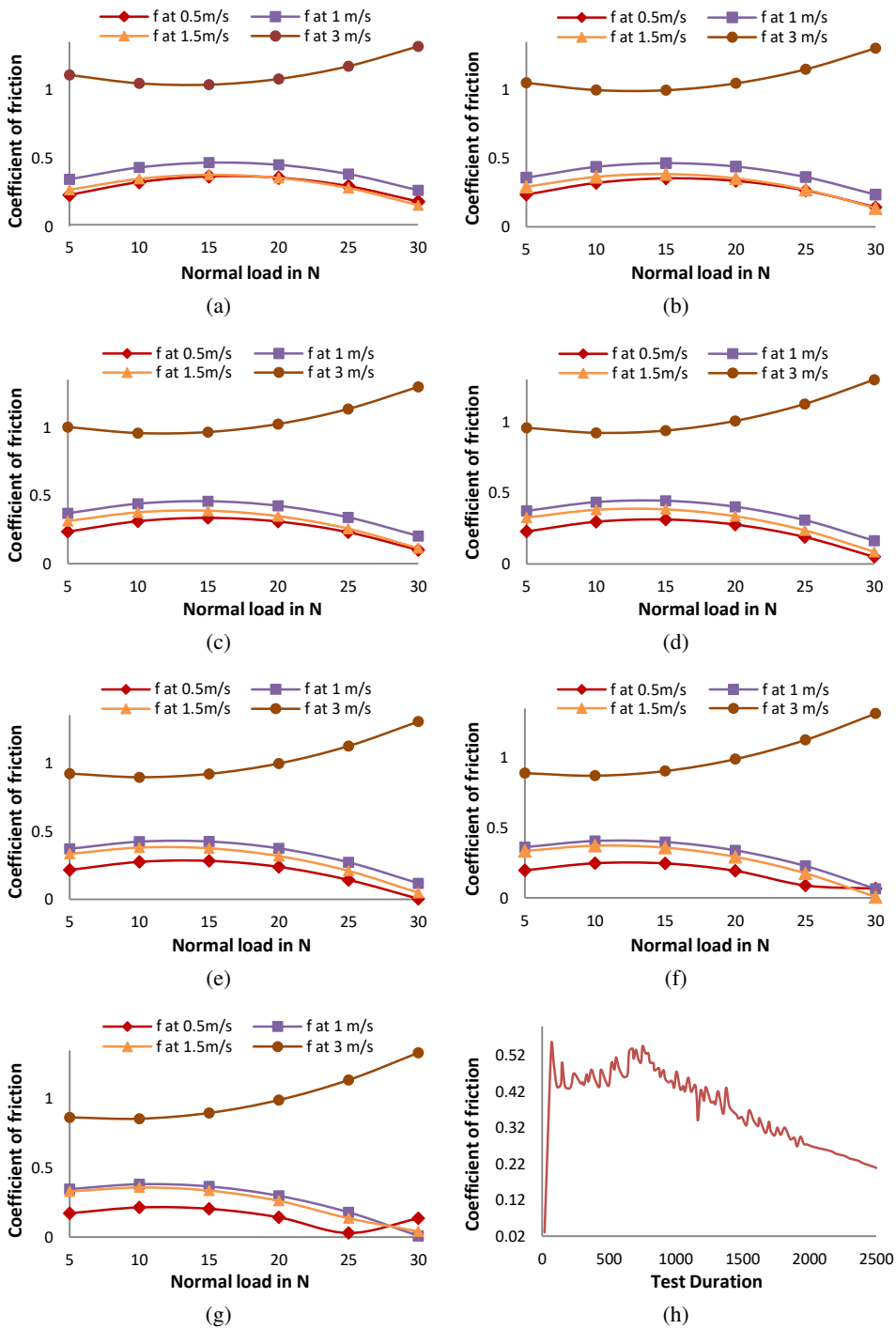
Fig. 2. COF vs NL at: (a) $0°$; (b) $15°$; (c) $30°$; (d) $45°$; (e) $60°$; (f) $75°$; (g) $90°$, and (h) duration of test

reduce the COF and it was noticed that COF had the lowest value at a low NL when the FDM sample pin was built with either very low or high PBO. This phenomenon happens because the NL on the sample pin is resisted by filaments/threads between the layers and within a layer of the FDM sample at smaller PBO. However, it fails with the increase of NL applied on the FDM filaments deposited on the horizontal build plane, where the threads/filaments between the layers fail to take this NL, which results in parting the threads/filaments [24]. Therefore, it causes a higher COF. For the same increase in NL, when the threads/filaments are deposited along the vertical direction, the filaments within the layers resist the entire NL.

When the PBO $\geqslant 75°$ and at a higher NL, the COF starts rising at a lower V of the wheel as threads/filaments within the layer that resist the load get stuck and exhibit no coordination in bearing the NL, which causes an increase in COF.

3.2. Wear-out rate (W_r)

Figs 3a–3g show the impact of the NL in combination with varying V of the wheel for each level of PBO on W_r of the FDM samples. With increasing NL, the W_r decreases only at NL lower levels up to 20 N, which is common for polymers. With increasing PBO, the W_r decreases steadily and then stabilizes, as the voids at low values of PBO are more predominant at lower orientation values and at the end section of neighboring thread/filament, which eventually fills [24]. Examining the figures of W_r for separately considered NL, V, and PBO, one can see a major impact of these quantities on W_r compared to the case of combined impact of V with factor PBO which were seen more predominant on W_r. Beyond a NL value of 20 N, the W_r starts rising indefinitely, because the material loses the strength to withstand continuous forming of asperities on the pin sample, which leads to an excessive W_r [23].

Figs 3a–3g show that the W_r has the lowest value when the PBO has its optimal value at either a high or low V value of the wheel. Regardless of the V value of the wheel, the minimum W_r is found at any value of the PBO lying between 25 to 38°, and at a low value of the PBO. However, when the sample is formed by the deposition of the substance alongside the building plane, the W_r is found to be high. When the PBO approaches 0°, irrespective of high or low NL, the similar distribution of results from Figs 3a–3g shown W_r is uniform and optimal as the filaments will be along the build plane [9]. Commonly, the W_r is high because of the low surface quality (due to higher Ra), which leads to a fracturing of the FDM sample [11]. This consequently increases the COF because the worn-out material of the sample pin stuck in the form of freed asperities could be retained as another item under wear along with sample pin and steel wheel. These additional stuck particles on the worn-out surfaces are dominant at the contacting surfaces and their increasing quantity attached to high spots developed at the wheel surface is subjected to plowing stroke on the wear pathways of the pin [19]. A continuous plowing stroke happens even during the remaining sliding motion of the wheel, and
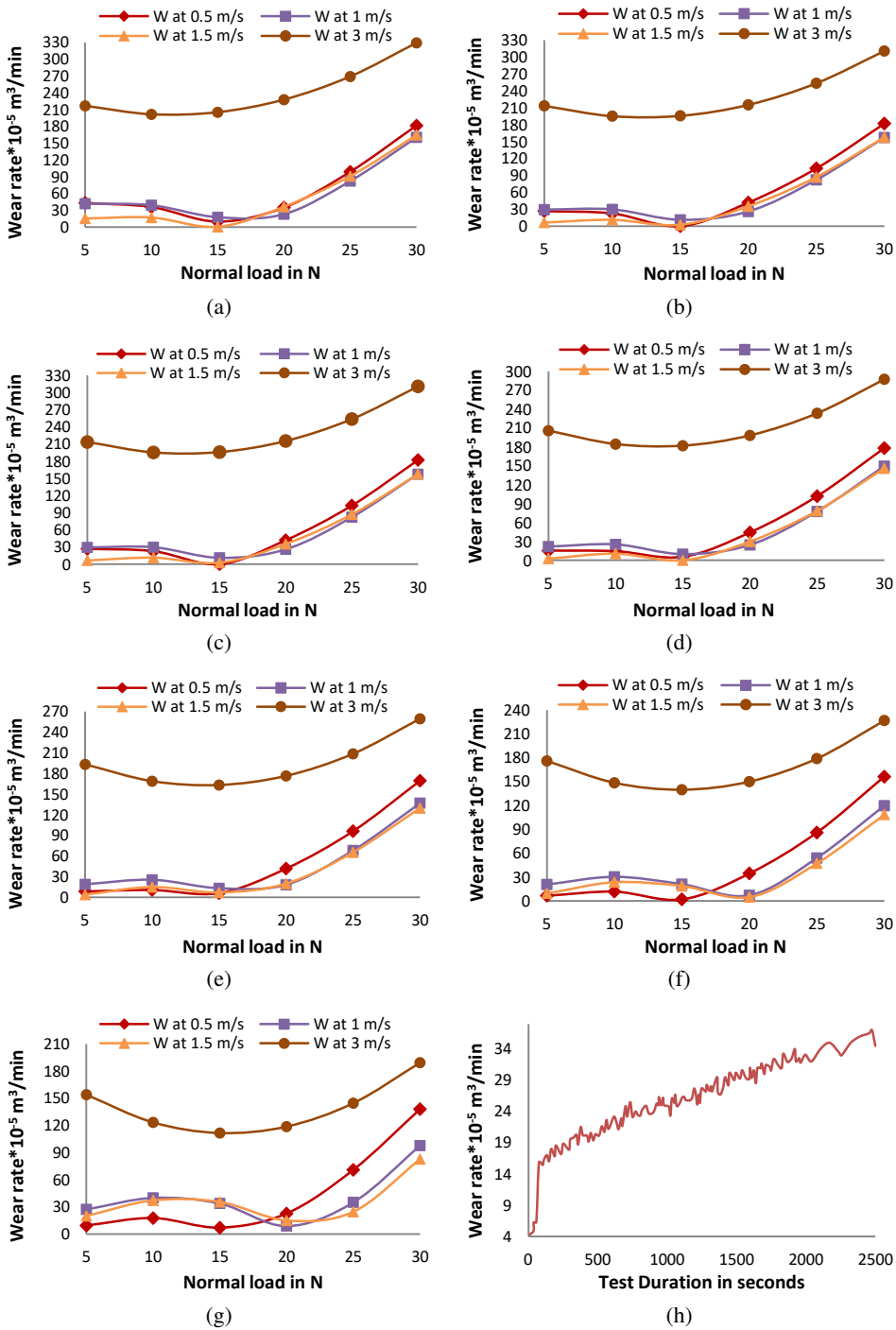
Fig. 3. Wear rate of FDM pin vs NL at: (a) 0°; (b) 15°; (c) 30°; (d) 45°; (e) 60°; (f) 75°; (g) 90°, and (h) test duration

it makes the W_r uniform for the complete duration of the test. Plowing substances get crumpled and then change into a powder form. This powder then gathers on both the sample pin and the wheel. A sudden drop in W_r indicates that the plowing stroke plays a dominant role. Fig. 3h shows the test results of the W_r versus total trial time, where wear-out starting from a lower value suddenly increases to a peak value and then W_r becomes stable. This can be explained similarly as with respect to COF. The high spots present at the interface between the wheel and the pin initially allow W_r to raise from zero to their peak value [20].

4. Conclusions

Polymers FDM parts are widely used in dry sliding circumstances and their tribological characteristics, namely W_r and COF, are used to evaluate designing plan of manufacturing techniques to be adopted. This paper examined the impacts of the FDM and tribological input elements on the sample pins made of polymer formed via the FDM process. Three input parameters, namely, NL, V and PBO (the FDM parameter) were chosen. The combined role of NL and V at various part building inclination ($0°$ to $90°$) on the COF and W_r were examined. The various inferences used in experimental work on TC are as follows:

- The PBO (orientation factor) decreases for a given NL and V of a wheel shift prior the cross-section of threads/filaments of a pin sample resulting in a high COF. The W_r of pins is also affected mainly through the V of wheel and the PBO at the time of building pin samples through the FDM means.
- With the increasing load, cracks are developed between the strings/ filaments resulting in shifting the V of the wheel prior the cross-section of fibers of a pin sample and high COF. Likewise, the NL at various inclinations affects the wear considerably, as seen in the COF.
- For the suitable W_r conditions, the desired PBO should be vertical or $90°$ for the filament deposition process and PBO should be $0°$ or horizontal at the low value of NL.
- The COF and W_r were substantially impacted when NL and V of the wheel were considered with the varying PBOs.
- Various PBO values were suggested for building the part while operating at lower/higher NLs and V or lower friction.
- A combination of a lower NL with higher V and an intermediate inclinations needed to achieve constant wear-out conditions as the filaments of surfaces/layers at low PBOs were found along the surface of the building platform.
- Various critical tribology conditions for enhancing the strength of FDM parts in machine components are suggested.
- Cracks formed in the samples when retested at high NL, high V, and low PBO while building the part in the FDM process.

- FDM parts with the lowest value of PBO bear a minimal NL between the layers. In contrast, at maximum PBO, the load is borne by filaments within layers which withstand maximum NL under uniform wear requirements.
- Prior studies revealed that the interaction between NL and PBO, and the interaction level between V and PBO are the predominant factors influencing wear rate, while the interaction level between factors V and PBO mostly influences friction.

This research can be improved upon in future work by developing regression models using analysis of variance, developing a more sophisticated multi-objective optimization requirements using a response surface, particle swarm, and fuzzy logic techniques.

A. Appendix

At PBO = $0°$

Normal Load, N	COF at V=0.5 m/s	COF at V=1 m/s	COF at V=1.5 m/s	COF at V=3 m/s
5	0.2292	0.343725	0.267175	1.108775
10	0.3228	0.4309	0.347925	1.0473
15	0.3648	0.466425	0.377025	1.037475
20	0.3551	0.4503	0.354475	1.0793
25	0.2937	0.382525	0.280275	1.172775
30	0.1807	0.2631	0.154425	1.3179
Normal Load, N	W_r at V=0.5 m/s	W_r at V=1 m/s	W_r at V=1.5 m/s	W_r at V=3 m/s
5	64.15	58.925	28.4	214.975
10	53.85	53.1	27.05	202.9
15	24.7	28.425	6.85	209.675
20	23.3	15.1	32.2	235.3
25	90.15	77.475	90.1	279.775
30	175.85	158.7	166.85	343.1

At PBO = $15°$

Normal Load, N	COF at V=0.5 m/s	COF at V=1 m/s	COF at V=1.5 m/s	COF at V=3 m/s
5	0.235428	0.359955	0.293433	1.052435
10	0.320403	0.438505	0.365558	0.999585
15	0.353728	0.465405	0.386033	0.998385
20	0.335403	0.440655	0.354858	1.048835
25	0.265428	0.364255	0.272033	1.150935
30	0.143803	0.236205	0.137558	1.304685

At PBO = 15°

Normal Load, N	W_r at V=0.5 m/s	W_r at V=1 m/s	W_r at V=1.5 m/s	W_r at V=3 m/s
5	43.15675	41.79425	15.13175	216.6558
10	35.94675	39.05925	16.87175	201.4908
15	9.88675	17.47425	0.23825	205.1758
20	35.02325	22.96075	36.19825	227.7108
25	98.78325	82.24575	91.00825	269.0958
30	181.3933	160.3808	164.6683	329.3308

At PBO = 30°

Normal Load, N	COF at V=0.5 m/s	COF at V=1 m/s	COF at V=1.5 m/s	COF at V=3 m/s
5	0.23533	0.369885	0.31339	1.002395
10	0.31168	0.43981	0.37689	0.95817
15	0.33638	0.458085	0.38874	0.965595
20	0.30943	0.42471	0.34894	1.02467
25	0.23083	0.339685	0.25749	1.135395
30	0.10058	0.20301	0.11439	1.29777
Normal Load, N	W_r at V=0.5 m/s	W_r at V=1 m/s	W_r at V=1.5 m/s	W_r at V=3 m/s
5	26.902	29.402	6.602	213.598
10	22.782	29.757	11.432	195.343
15	0.188	11.262	2.588	195.938
20	42.008	26.083	35.458	215.383
25	102.678	82.278	87.178	253.678
30	182.198	157.323	157.748	310.823

At PBO = 45°

Normal Load, N	COF at V=0.5 m/s	COF at V=1 m/s	COF at V=1.5 m/s	COF at V=3 m/s
5	0.228933	0.373515	0.327048	0.958655
10	0.296658	0.434815	0.381923	0.923055
15	0.312733	0.444465	0.385148	0.939105
20	0.277158	0.402465	0.336723	1.006805
25	0.189933	0.308815	0.236648	1.126155
30	0.051057	0.163515	0.084922	1.297155
Normal Load, N	W_r at V=0.5 m/s	W_r at V=1 m/s	W_r at V=1.5 m/s	W_r at V=3 m/s
5	15.38575	2 1.74825	2.81075	205.8018
10	14.35575	25.19325	10.73075	184.4568
15	5.52425	9.78825	0.19925	181.9618
20	44.25425	24.46675	29.97925	198.3168
25	101.8343	77.57175	78.60925	233.5218
30	178.2643	149.5268	146.0893	287.5768

At PBO = 60°

Normal Load, N	COF at V=0.5 m/s	COF at V=1 m/s	COF at V=1.5 m/s	COF at V=3 m/s
5	0.216235	0.370845	0.334405	0.921215
10	0.275335	0.42352	0.380655	0.89424
15	0.282785	0.424545	0.375255	0.918915
20	0.238585	0.37392	0.318205	0.99524
25	0.142735	0.271645	0.209505	1.123215
30	0.004765	0.11772	0.049155	1.30284
Normal Load, N	W_r at V=0.5 m/s	W_r at V=1 m/s	W_r at V=1.5 m/s	W_r at V=3 m/s
5	8.608	18.833	3.758	193.267
10	10.668	25.368	14.768	168.832
15	6.122	13.053	6.928	163.247
20	41.762	18.112	19.762	176.512
25	96.252	68.127	65.302	208.627
30	169.592	136.992	129.692	259.592

At PBO = 75°

Normal Load, N	COF at V=0.5 m/s	COF at V=1 m/s	COF at V=1.5 m/s	COF at V=3 m/s
5	0.197238	0.361875	0.335463	0.890075
10	0.247713	0.405925	0.373088	0.871725
15	0.246538	0.398325	0.359063	0.905025
20	0.193713	0.339075	0.293388	0.989975
25	0.089237	0.228175	0.176063	1.126575
30	0.066888	0.065625	0.007088	1.314825
Normal Load, N	W_r at V=0.5 m/s	W_r at V=1 m/s	W_r at V=1.5 m/s	W_r at V=3 m/s
5	6.56875	20.65625	9.44375	175.9938
10	11.71875	30.28125	23.54375	148.4688
15	1.98125	21.05625	18.79375	139.7938
20	34.53125	7.01875	4.80625	149.9688
25	85.93125	53.94375	47.25625	178.9938
30	156.1813	119.7188	108.5563	226.8688

At PBO = 90°

Normal Load, N	COF at V=0.5 m/s	COF at V=1 m/s	COF at V=1.5 m/s	COF at V=3 m/s
5	0.17194	0.346605	0.33022	0.865235
10	0.21379	0.38203	0.35922	0.85551
15	0.20399	0.365805	0.33657	0.897435
20	0.14254	0.29793	0.26227	0.99101
25	0.02944	0.178405	0.13632	1.136235
30	0.13531	0.00723	0.04128	1.33311

At PBO = $90°$

Normal Load, N	W_r at V=0.5 m/s	W_r at V=1 m/s	W_r at V=1.5 m/s	W_r at V=3 m/s
5	9.268	27.218	19.868	153.982
10	17.508	39.933	37.058	123.367
15	6.898	33.798	35.398	111.602
20	22.562	8.813	14.888	118.687
25	70.872	35.022	24.472	144.622
30	138.032	97.707	82.682	189.407

References

[1] D. Ahn, J.-H. Kweon, S. Kwon, J. Song, and S. Lee. Representation of surface roughness in fused deposition modeling. *Journal of Materials Processing Technology*, 209(15-16):5593–5600, 2009. doi: 10.1016/j.jmatprotec.2009.05.016.

[2] C.K. Chua, S.H. Teh, and R.K.L. Gay. Rapid prototyping versus virtual prototyping in product design and manufacturing. *The International Journal of Advanced Manufacturing Technology*, 15(8):597–603, 1999. doi: 10.1007/s001700050107.

[3] W. Zeng, F. Lin, T. Shi, R. Zhang, Y. Nian, J. Ruan, and T Zhou. Fused deposition modelling of an auricle framework for microtia reconstruction based on CT images. *Rapid Prototyping Journal*, 15(5):280–284, 2008. doi: 10.1108/13552540810907947.

[4] S.H. Choi and H.H. Cheung. Multi-material virtual prototyping for product development and biomedical engineering. *Computers in Industry*, 58(5):438–452, 2007. doi: 10.1016/j.compind.2006.09.002.

[5] E.C. Santos, M. Shiomi, K. Osakada, and T. Laoui. Rapid manufacturing of metal components by laser forming. *International Journal of Machine Tools and Manufacture*, 46(12-13):1459–1468, 2006. doi: 10.1016/j.ijmachtools.2005.09.005.

[6] N. Oxman. Variable property rapid prototyping. *Virtual and Physical Prototyping*, 6(1):3–31, 2011. doi: 10.1080/17452759.2011.558588.

[7] A. Bellini, L. Shor, and S.I. Guceri. New developments in fused deposition modeling of ceramics. *Rapid Prototyping Journal*, 11(4):214–220, 2005. doi: 10.1108/13552540510612901.

[8] K.D. Dearn, T.J. Hoskins, D.G. Petrov, S.C. Reynolds, and R. Banks. Applications of dry film lubricants for polymer gears. *Wear*, 298-299:99–108, 2013. doi: 10.1016/j.wear.2012.11.003.

[9] S.E. Franklin. Wear experiments with selected engineering polymers and polymer composites under dry reciprocating sliding conditions. *Wear*, 251(1-12):1591–1598, 2001. doi: 10.1016/S0043-1648(01)00795-5.

[10] P.V. Vasconcelos, F.J. Lino, A.M. Baptista, and R.J. Neto. Tribological behaviour of epoxy based composites for rapid tooling. *Wear*, 260(1-2):30–39, 2006. doi: 10.1016/j.wear.2004.12.030.

[11] B.-B. Jia, T.-S. Li, X.-J. Liu, and P.-H. Cong. Tribological behaviors of several polymer–polymer sliding combinations under dry friction and oil-lubricated conditions. *Wear*, 262(11-12):1353–1359, 2007. doi: 10.1016/j.wear.2007.01.011.

[12] A. Equbal, A.K. Sood, V. Toppo, R.K. Ohdar, and S.S. Mahapatra. Prediction and analysis of sliding wear performance of fused deposition modelling-processed ABS plastic parts. *Proceedings of the Institution of Mechanical Engineers, Part J: Journal of Engineering Tribology*, 224(12):1261–1271, 2010. doi: 10.1243/13506501JET835.

[13] A. Pereira, J. Pérez, J. Diéguez, G. Peláez, and J. Ares. Design and manufacture of casting pattern plates by rapid tooling. *Archives of Material Science*, 29(1-2):63–67, 2008.

[14] Q. Liu, M.C. Leu, and S.M. Schmitt. Rapid prototyping in dentistry: technology and application. *The International Journal of Advanced Manufacturing Technology*, 29(3):317–335, 2006. doi: 10.1007/s00170-005-2523-2.

[15] T. Brajlih, B. Valentan, J. Balic, and I. Drstvensek. Speed and accuracy evaluation of additive manufacturing machines. *Rapid Prototyping Journal*, 17(1):64–75, 2011. doi: 10.1108/13552541111098644.

[16] Y. Yan, S. Li, R. Zhang, F. Lin, R. Wu, Q. Lu, Z. Xiong, and X. Wang. Rapid prototyping and manufacturing technology: principle, representative technics, applications, and development trends. *Tsinghua Science and Technology*, 14(S1):1–12, 2009. doi: 10.1016/S1007-0214(09)70059-8.

[17] P. Rochus, J.-Y. Plesseria, M. Van Elsen, J.-P. Kruth, R. Carrus, and T. Dormal. New applications of rapid prototyping and rapid manufacturing (RP/RM) technologies for space instrumentation. *Acta Astronautica*, 61(1-6):352–359, 2007. doi: 10.1016/j.actaastro.2007.01.004.

[18] Z. Rymuza, Z. Kusznierewicz, T. Solarski, M. Kwacz, S.A. Chizhik, and A.V. Goldade. Static friction and adhesion in polymer–polymer microbearings. *Wear*, 238(1):56–69, 2000. doi: 10.1016/S0043-1648(99)00341-5.

[19] M.M. Hanon, Y. Alshammas, and L. Zsidai. Effect of print orientation and bronze existence on tribological and mechanical properties of 3D-printed bronze/PLA composite. *The International Journal of Advanced Manufacturing Technology*, 108:553–570, 2020. doi: 10.1007/s00170-020-05391-x.

[20] M.N.M. Norani M.I.H.C. Abdullah, M.F.B. Abdollah, H. Amiruddin, F.R. Ramli, and N. Tamaldin. Tribological analysis of a 3D-printed internal triangular flip ABS pin during running-in stage. *Jurnal Tribologi*, 27:42–56, 2020.

[21] G.S. Balan, V.S. Kumar, S. Rajaram, and M. Ravichandran. Investigation on water absorption and wear characteristics of waste plastics and seashell powder reinforced polymer composite. *Jurnal Tribologi*, 27:57–70, 2020.

[22] M. Yunus and M.S. Alsoufi. Effect of raster inclinations and part positions on mechanical properties, surface roughness and manufacturing price of printed parts produced by fused deposition method. *Journal of Mechanical Engineering and Sciences*, 14(4):7416–7423, 2020. doi: 10.15282/jmes.14.4.2020.10.0584.

[23] M. Yunus and M.S. Alsoufi. Experimental investigations into the mechanical, tribological, and corrosion properties of hybrid polymer matrix composites comprising ceramic reinforcement for biomedical applications. *International Journal of Biomaterials*, 2018:ID9283291, 2018. doi: 10.1155/2018/9283291.

[24] P.K. Gurrala and S.P. Regalla. Friction and wear behavior of abs polymer parts made by fused deposition modeling (FDM). *Technology Letters*, 1(12):13–17, 2014.